Coseismic indentor-related deformation during the termination of subduction and its associated geophysical characteristics: An example from Taiwan

Wu-Cheng Chi*
INSTITUTE OF EARTH SCIENCES, ACADEMIA SINICA, 128 ACADEMIA ROAD, SEC 2, NANKANG, TAIPEI 115, TAIWAN

ABSTRACT

Collision is among the important processes for the growth of continents, and the way in which subduction becomes a collision is still an active research topic. Here, I examine the seismogenic structures of southern and central Taiwan where the subduction along the Manila Trench has terminated and given way to an arc-continent collision on land. Based on focal mechanisms and seven finite-fault slip models, coseismic tectonic extrusion is active in this region, in which the basement highs on the incoming passive margin are acting as indentors and strongly modifying the seismic moment release patterns in the collision zone. At least three magnitude 7 earthquakes have ruptured both north and south of an indentor called the Peikang high in the past hundred years. After examination, the basement highs show little global positioning system (GPS)–recorded relative motion with respect to the incoming passive margin; high Bouguer gravity anomalies associated with denser materials of the basement; and low heat flow due to less dewatering and exhumation. With regard to seismogenic structures, faster GPS relative motions, lower Bouguer gravity anomalies, and higher heat flow characterize the regions surrounding the indentors. Similar processes might be operating in other arc-continent collision zones. For other regions where there are fewer seismic instruments to monitor earthquakes, it might be helpful to combine a geological survey with gravity and other geophysical data sets to help identify such potential seismogenic structures.

LITHOSPHERE; v. 4; no. 6; p. 594–602 | Published online 2 October 2012 doi: 10.1130/L193.1

INTRODUCTION

Crustal deformation styles change when subduction terminates and becomes a collision. Some of these structural changes have been successfully documented by studying surface geology and other data sets (Silver et al., 1983; Teng, 1990; Abers and McCaffrey, 1994; Wu et al., 1997; Brown et al., 1998; Draut and Clift, 2001; Kao et al., 2001; Malavieille et al., 2002; Dilek et al., 2010). In the study of many mature collision zones, the map-view tectonic extrusion model is a leading hypothesis (e.g., Peltzer and Tapponnier, 1988; Houseman and England, 1993) used to explain observed collisional features; however, it is still unclear whether and how such process can occur coseismically, and whether smaller-scale (tens of kilometers) indentors can cause map-view extrusion in a style similar to that of the continental scale. It is also not clear if there are geophysical features that can be correlated with these potential earthquake rupture zones. These questions are important for seismic hazard analysis purposes. Here, recently published earthquake waveform modeling results are used to interpret seismogenic structural patterns of an arc-continent collision in the Taiwan region where the subduction zone terminates as a result of the arrival of the thick and buoyant continental passive margin at the convergence zone.

The incoming passive margin basement is composed of horsts and grabens, which were formed by many strike-slip and normal faults. These steep preexisting, or subvertical weak zones appear to have been reactivated in the collision zone, thus complicating the seismogenic structures due to the preexisting weak fault surfaces. In particular, the basement highs can act as indentors that influence the style of coseismic energy release. Also included will be a discussion about the ways in which global positioning system (GPS), gravity, and heat-flow data sets can be used to help interpret these high seismic hazard zones in other collision zones.

REGIONAL TECTONIC SETTING

Taiwan is located along the boundary between the Eurasian and Philippine Sea plates. To the south, the oceanic lithosphere of the South China Sea is subducting eastward beneath the Philippine Sea plate (Bowin et al., 1978) with a high rate of 7–9 cm/yr (e.g., Yu et al., 1997). To the north, the subduction terminates and changes into arc-continent collision where the Chinese passive margin enters into the convergence zone (McIntosh et al., 2005). Thus, in map view, Taiwan captures an along-strike transition from subduction of oceanic lithosphere to collision of a passive margin with the same convergence zone, with the resultant termination of subduction (Fig. 1). Currently, the rate of southward propagation of the Taiwan collision zone along the convergent boundary ranges from 55 to 90 mm/yr (Suppe, 1984; Byrne and Liu, 2002; Willett et al., 2003).

Along the subduction zone, the mid-ocean ridge of the South China Sea plate used to spread in a NW-SE direction (Briais et al., 1993). To the north in the collision zone, the Chinese passive margin has NE-SW–striking normal faults dipping to the SE and NW (Liu et al., 1997; Hsu et al., 2004). Some of the normal faults are linked by NNW-SSE–striking transfer faults. Some of the normal faults are deep rooted (Nissen et al., 1995; Wang et al., 2006). Based on gravity modeling, Nissen et al. (1995) documented Moho-cutting fault structures along a passive margin transect west of Taiwan. Near Taiwan, the

*E-mail: wchi@gate.sinica.edu.tw.

Editor's note: This article is part of a special issue titled "Initiation and Termination of Subduction: Rock Record, Geodynamic Models, Modern Plate Boundaries," edited by John Shervais and John Wakabayashi. The full issue can be found at http://lithosphere.gsapubs.org/content/4/6.toc.

continental shelf shows more complex structures, including horsts and grabens that generate basement highs and thick sedimentary strata. There are two basement highs on the incoming plate west of Taiwan: the Peikang high and Kuanyin high. Lin et al. (2003) published a basement map, showing these basement highs. Lu et al. (2002) also interpreted the influence of the basement highs on the curvatures of the fault traces in the overriding plate in this region (Fig. 2). Recently, Byrne et al. (2011) discussed in detail how such basement highs affect mountain-building processes. They proposed that the basement highs and the basins surrounding them are results of spreading direction changes. These structures on the incoming plate can influence the deformation on the overriding plate.

The deformation styles of the overriding plate also vary from subduction to collision. The subduction zone includes a well-developed accretionary prism, forearc basin, and arc. The accretionary prism can be classified into three domains (Reed et al., 1992). The lower slope domain near the trench shows typical fold-and-thrust structures. The upper slope domain is transparent in seismic profiles, suggesting intense deformation or subvertical strata. The back-thrust domain lies along the boundary between the accretionary prism and the forearc basin where a tectonic wedging process is active (Chi et al., 2003). The forearc strata are subparallel, some with mass-wasting deposits (Yen and Lundberg, 2006), at least at shallow depths. The arc is subparallel to the trench with a constant distance of ~120 km in the subduction zone, but the distance decreases where the subduction zone terminates near Taiwan, and the forearc basin is consumed in the collision zone.

The island of Taiwan is located in a mature collision zone. From west (foreland) to east (hinterland), there are six geological units: Coastal Plains, Western Foothills, Hsuehshan Range, Central Range, Longitudinal Valley, and Coastal Range. The Coastal Plain contains passive margin structures overlain by a vast amount of sediments eroded from the east since the time the collisional mountain-building process has been active. In the Western Foothills, the thrusts show curvatures with wavelengths of ~100 km. Some of the thrusts are connected by transfer faults. The Hsuehshan Range is interpreted as a pop-up structure from reactivation of normal faults bounded by a previous graben (Teng, 1990). The Central Range is the northern extension of the upper slope domain of the offshore Taiwan accretionary prism. The Longitudinal Valley is the northern extension of the consumed forearc basin, and it has taken up at least half of the current 7–9 cm/yr interseismic shortening across this convergence zone (Yu et al., 1997).

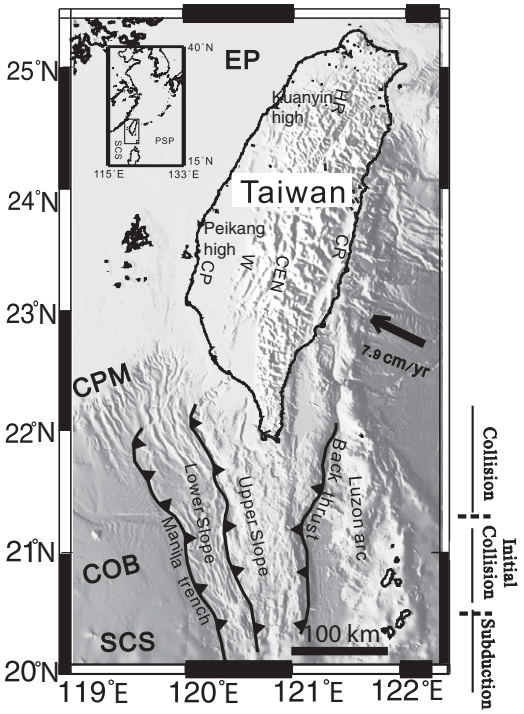

Figure 1. Map of Taiwan. To the south, the South China Sea (SCS) plate is subducting under the Philippine Sea plate (PSP) with a relative motion of 7–9 cm/yr, forming the Manila Trench, Taiwan accretionary prism, forearc basin, and the Luzon arc. The offshore Taiwan accretionary prism is composed of the lower slope domain, upper slope domain, and the back-thrust domain. North of the continent-ocean boundary (COB), the subduction becomes a collision, and forms the island of Taiwan where the Chinese passive margin (CPM) enters into the convergence zone. There are several geological provinces in Taiwan. From west (foreland) to east (hinterland), they include: the Coastal Plains (CP), Western Foothills (W), Hsuehshan Range (HR), Central Range (CEN), and Coastal Range (CR).

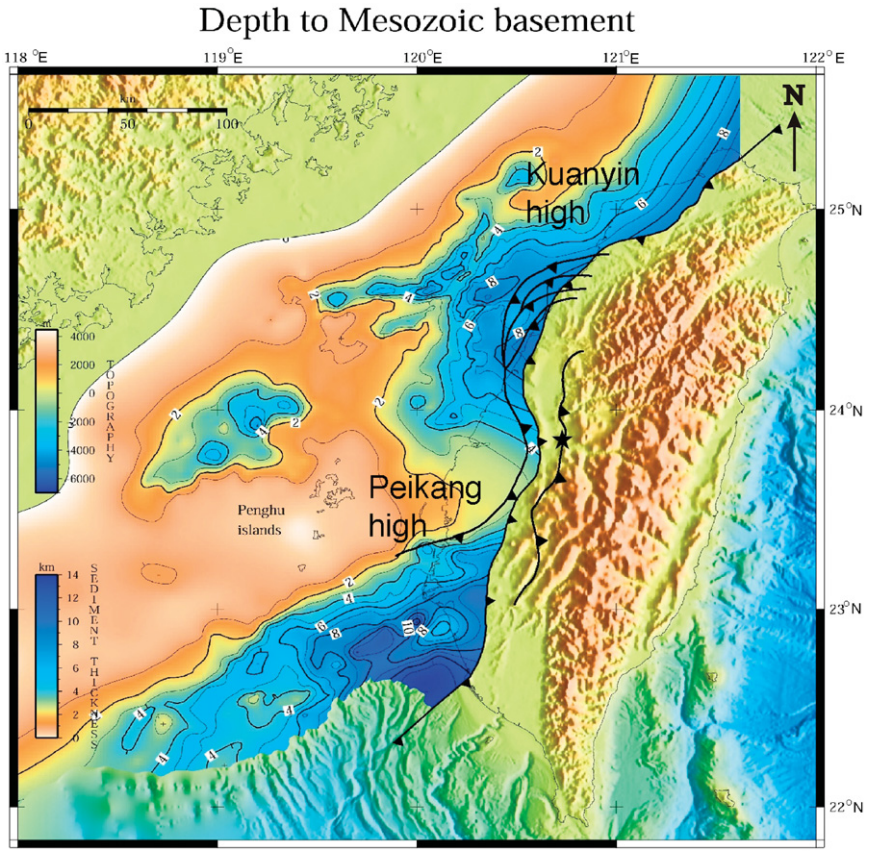

Figure 2. Mesozoic basement map of Taiwan (modified after Lin et al., 2003). The sediment thickness data in the foreland are compiled from a large number of oil wells. We have plotted the thrusts in the foreland region. Note the location of the Peikang and Kuanyin highs. These two basement highs, or indentors, have influenced the curvature of the fault traces (Lu et al., 2002). The star shows the hypocenter of the 1999 Chi-Chi, Taiwan, earthquake.

The Coastal Range is an accreted volcanic arc. Based on paleomagnetic data, the arc was segmented and rotated clockwise when it entered the collision zone (Lee et al., 1991). There is no morphological evidence of a forearc basin in the collision zone (Lundberg et al., 1997), where the collided arc is juxtaposed directly against the Central Range of Taiwan.

Due to the oblique plate-boundary configuration in the Taiwan region, different stages of subduction and collision occur simultaneously along the strike of the convergent boundary. As a result, the evolution of seismogenic structures can be studied based upon evidence from the younger subduction zone to the south to the collision zone to the north. In particular, we are interested in determining if there are unique seismogenic structures that are associated with the termination of the subduction in the mature collision zone in Central Taiwan, where the basement highs along the passive margin have entered into the convergence zone as indentors.

RECENT RESULTS ON SEISMOGENIC STRUCTURES OF TAIWAN

In this study, I will mainly use two seismic data sets derived from our group. The first data set was published recently (Chang et al., 2011) and is based upon a new procedure we developed to invert moment tensor solutions using Taiwan's excellent strong motion waveform data. The second data set is from our previous work on finite-fault inversions of the Chi-Chi main shock and its large aftershocks (Chi et al., 2001; Chi and Dreger, 2002; Chi and Dreger, 2004). The reliability of these two data sets has been carefully documented and rigorously reviewed in our previous work. In addition, another moment tensor catalog (e.g., Kao et al., 2001) derived from data from a regional broadband network (BATS) will also be discussed briefly. Because these solutions are constrained by full waveforms, these solutions are usually considered of higher reliability. In this work, I will focus on geological and geophysical interpretation of these data sets and correlate them with other available geophysical data in order to study the seismogenic structures where the subduction terminates.

We (Chang et al., 2011) inverted strong motion waveforms to derive moment tensors of many Mw >4.8 and greater earthquakes since 1993. In the 2011 paper, a new procedure used to derive the solutions was documented. Here, I will discuss the interpretation of these solutions. This catalog covers a large portion of the seismic moment release in this region (Fig. 3). Overall, the maximum compressive stress (sigma 1) direction is subparallel with the plate convergence direction, except in regions where the arc starts to dock and rotate along the passive margin.

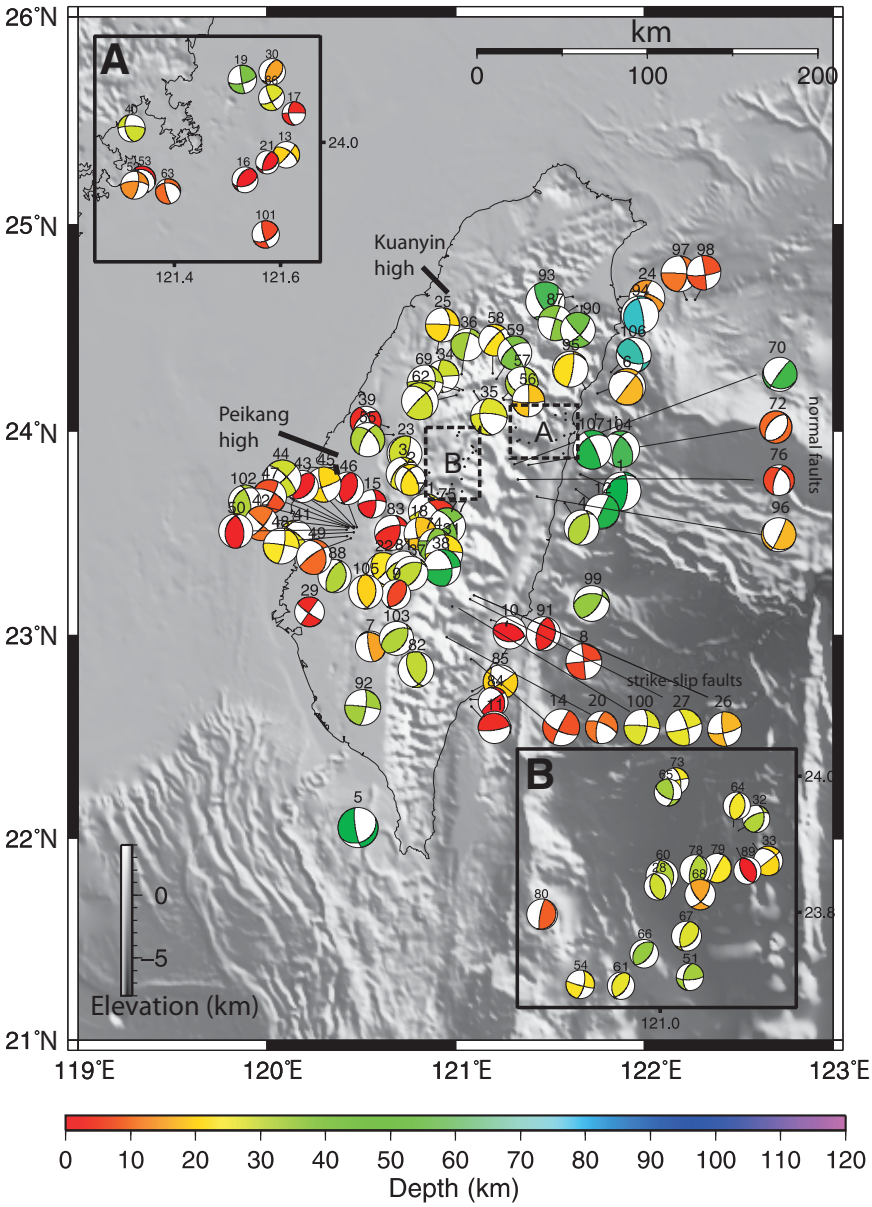

Figure 3. The focal mechanisms derived from our recent study (Chang et al., 2011). There are diverse focal mechanisms in the foreland of the collision zone, mostly strike-slip and reverse as deep as 40 km. There are also shallow thrusts in the sediments deposited after erosion from the collisional mountain-building process to the east. In this study, I also document three features: (1) the strike-slip faults in the hinterland (eastern flank of the Central Range) at 23°N; (2) the normal faults in the hinterland at 24°N; and (3) an earthquake sequence in the Coastal Plains (earthquake numbers from 41 to 50). For detailed information of the earthquakes, check the numbers that are listed in Chang et al. (2011). Blocks A and B best show the focal mechanisms in regions of dense seismicity.

In the foreland region, including the Coastal Plains, Western Foothills, Hsuehshan Range, and western flank of the Central Range, there are diverse focal mechanisms from shallow depths down to the lower crust. Most of them reflect thrusts or reverse mechanisms, but there are also strike-slip faults. With the exception of the Chi-Chi main shock and some of its aftershocks, which we will discuss later, most of the dip-slip events are of relatively high angles and at greater depths, some as deep as 40 km. Lin and Roecker (1993) have also proposed a cluster of seismicity down to 60 km at latitude 24°N.

In the hinterland region, particularly the eastern flank of the Central Range, there are two groups of particular focal mechanisms. In the

south, between 23°N and 23.5°N, where the arc starts to collide with the passive margin, there are mostly strike-slip faults in the shallow to midcrust area. As the collision becomes more mature at 24°N, we see mostly normal faults in the hinterland.

This catalog also includes a 1999 earthquake sequence in Meishan in the foreland region under the Coastal Plains. This earthquake sequence, which occurred one month after the Chi-Chi main shock, is unique because there were two M 7 earthquakes that occurred in this region in 1906 (M_L 7.1) and in 1941 (M_L 7.1), causing substantial damage. A similar event now would cause much more damage due to the current dense population in this region. Several very different and conflicting seismogenic structures have been interpreted, including right-lateral, left-lateral strike-slip faults, and thrusts. From the catalog (Fig. 4), we found that this sequence is dominated by a NE-SW–trending strike-slip fault with reverse faults at the ends of the fault trace. Shyu et al. (2005) also interpreted the strike-slip fault as a transfer fault. This earthquake sequence ruptured the basement and occurred along the southern boundary of the Peikang high (Fig. 2). A month prior to this earthquake sequence, the Chi-Chi earthquake sequence ruptured to the north of the Peikang high.

We inverted finite-fault source models of the Chi-Chi earthquake and its large aftershocks (Chi et al., 2001; Chi and Dreger, 2002; Chi and Dreger, 2004). The main shock ruptured within a triangular region that is bounded by the Peikang and Kuanyin basement highs. During the earthquake sequence, two transfer faults were also identified (Kao and Chen, 2000; Chi and Dreger, 2004). From our finite-fault model, we found that at least one of the strike-slip faults ruptured in the basement at depth with a small moment release; thereafter, most of the moment release occurred above the décollement (Fig. 5).

A cross-section view (Fig. 6) shows that the Chi-Chi main shock ruptured on the ramp and flat of the décollement. There was another aftershock that ruptured on the flat. We identified a back thrust that ruptured above the décollement, and a reverse fault that ruptured from the décollement to the basement. As mentioned in the previous paragraph, the earthquake nucleated on a vertical strike-slip fault in the basement, but then ruptured upward, with most of the moment release occurring at shallow depth on the vertical transfer fault above the décollement. Kao and Chen (2000) interpreted this strike-slip fault as a transfer fault, similar to the lateral ramp of the thrusting on the décollement.

INTERPRETATIONS OF SEISMOGENIC STRUCTURES

The steeply dipping reverse faulting and subvertical strike-slip faulting in the mid- or lower crust suggest that these are reactivations of preexisting structures from the passive margin (Fig. 6). Some of the normal faults might have cut the lower crust as suggested by Nissen et al. (1995). In addition, there are new thrusts that developed in shallow sedimentary strata deposited during the collisional processes. However, even the shallow earthquake events are affected by the passive margin structures. For example, the strike-slip fault at a shallow depth is collocated with the strike-slip fault plane at basement

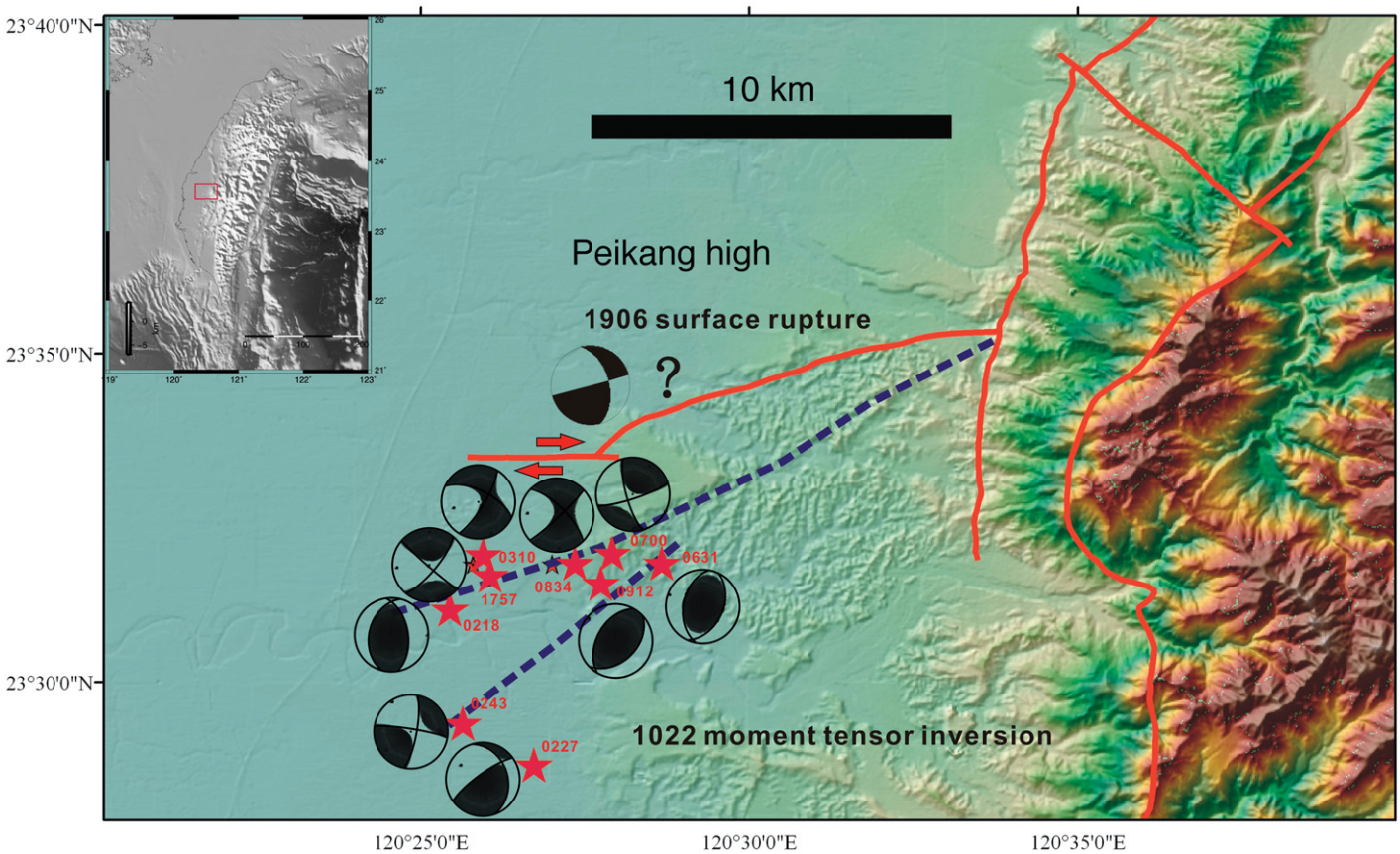

Figure 4. The locations and the focal mechanisms of the 22 October 1999 earthquake sequence. Previously, two early magnitude 7 earthquakes occurred in this region. The 1906 earthquake showed a possible surface rupture. We found the 22 October 1999 earthquake sequence rupture on a strike-slip fault plane and several reverse faults to the south of the strike-slip fault. The strike-slip fault is interpreted as a transfer fault (Shyu et al., 2005) bounded on the southern margin of the Peikang high.

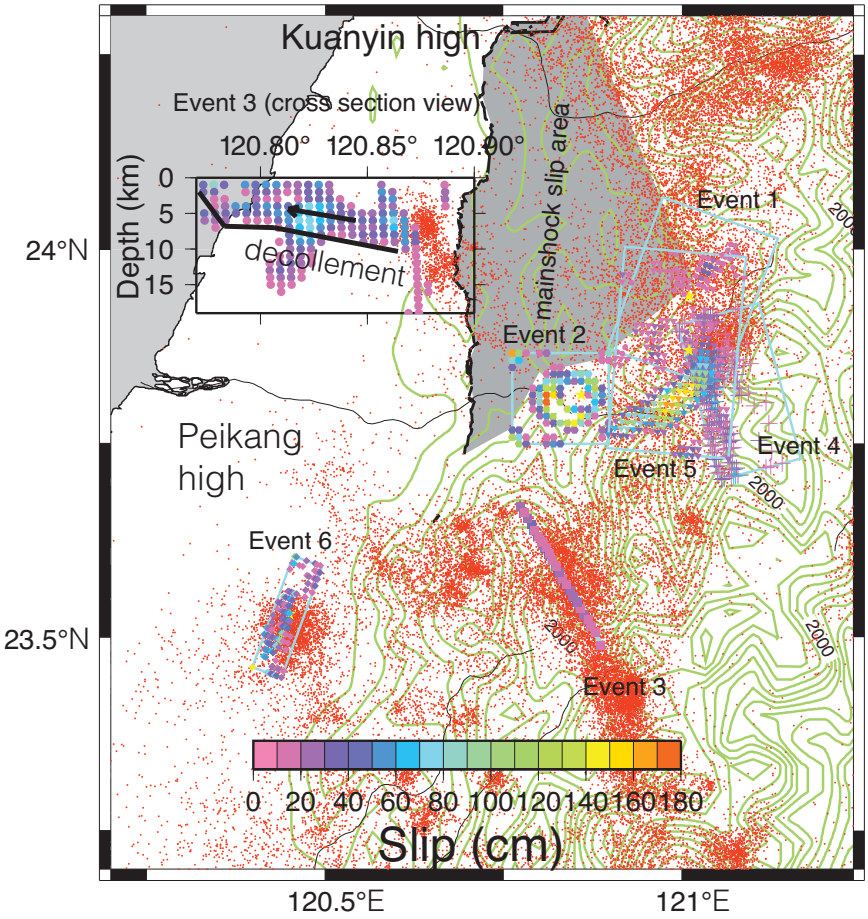

Figure 5. The map view of the finite-fault slip model of the 1999 Chi-Chi main shock and its six large aftershocks (Chi and Dreger, 2004). The color scale shows the amount of slip on the fault plane. Because the average main-shock slip is much larger than that of the aftershocks, only the main-shock slip area (Chi et al., 2001) is marked as the gray triangle area. The slips and the fault planes have been superimposed upon the topographic surface, which has a contour interval of 200 m. The event numbers for the six aftershocks are given in chronological order as listed in Chi and Dreger (2004). The red dots are small aftershocks. The main-shock slip area is located in a triangle zone that is bounded by the Peikang and Kuanyin highs. Most of the aftershocks are reverse faults. There is one strike-slip fault (event 3, marked as the purple line on map view, with its cross-sectional view of the slip model shown in the upper-left part of the figure) to the south that ruptured first in the basement at 15 km in depth, and showed large moment release not on the décollement, but above the décollement on a vertical strike-slip fault at shallow depth (see the event 3 cross-section view). The depth axis for the cross section is in km. The horizontal scale of the cross section is the same as the map-view plot, but the corresponding longitude is plotted as reference. In other words, the cross section is plotted parallel to the strike-slip fault. The main shock of the 22 October 1999 sequence (event 6) ruptured on an east-vergent fault in the basement.

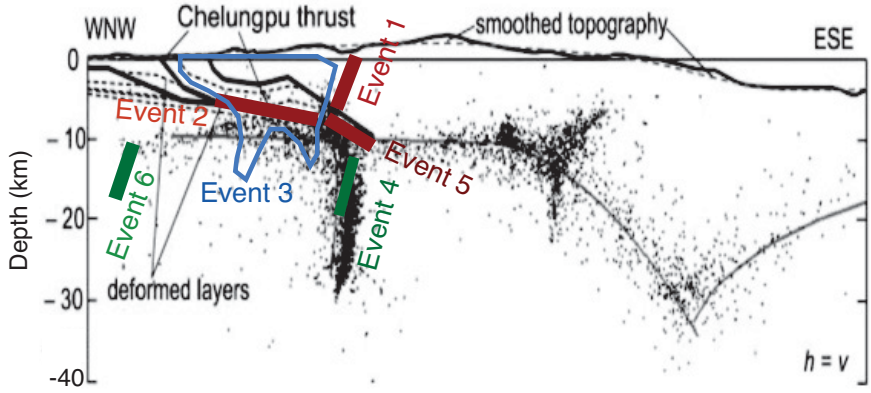

Figure 6. The cross-section view of the finite-fault slip models. The base seismicity map is based on Carena et al. (2002). The Chi-Chi main shock ruptured from the décollement to a ramp of an out-of-sequence fault called Chelungpu thrust. The red lines show the ruptured fault planes of the large Chi-Chi reverse and thrust aftershocks on the décollement and in the upper plate, the green lines show the ruptures in the lower plate, and the blue enclosed line shows the slip area of the strike-slip aftershock on a subvertical fault plane. One aftershock (event 1) ruptured on a back thrust above the décollement. Another aftershock (event 2) ruptured on the flat of the décollement. Event 4 then ruptured on a ramp at greater depth. The blue line encloses the strike-slip aftershock (event 3) that ruptured on the transfer fault. It nucleated in the basement before the major moment release above the décollement. A west-dipping fault (event 5) ruptured from the décollement to the basement. The green one on the westernmost side is the main shock (event 6) of the 22 October 1999 sequence.

depth. Also, the Chi-Chi main shock ruptured between the basement highs.

There are debates about whether seamounts (or other indentors) can act as asperities or barriers for earthquake ruptures (e.g., Tsumura et al., 2009; Wang and Bilek, 2011). In the case of Chi-Chi main shock, the basement highs acted as barriers that stopped the rupture of the main shock. The distance between the basement high thus defines the length of the earthquake rupture surface. Based on scaling relations, we can roughly estimate the size of the earthquake using the length of the earthquake rupture surface, i.e., distance between the basement highs, for seismic hazard estimates or earthquake simulation scenarios.

We found that the areas north and south of the Peikang high are capable of generating Mw 7 or greater earthquakes: Mw 7.6, 1999 Chi-Chi earthquake to the north, and M 7.1, 17 March 1906 Meishan earthquake and M 7.1, 17 December 1941 Chungpu earthquake to the south of the Peikang high. These large events can rupture on the strike-slip transfer faults or on the thrust

fault plane. In other words, in the case of Taiwan, the three-dimensional structures of the tectonic extrusion include the bounding strike-slip faults (or subvertical reverse faults) and a very shallow dipping thrust in between.

It is worth noting that the time span of these results is less than 100 yr and may not represent the total coseismic release patterns in this region over a longer time scale. However, the particular seismic release patterns reported in this study are related to the termination of the subduction and show at least part of the diverse deformation styles existing in such a tectonic setting.

RELATIONS BETWEEN SEISMOGENIC STRUCTURES AND OTHER GEOPHYSICAL DATA SETS

Both the Chi-Chi sequence and 22 October 1999 Meishan sequence are related to the Peikang high, which acts as an indentor to cause the coseismic tectonic extrusion. Next, this paper will explore hints in other geophysical data sets that can help to identify such indentors and the associated high seismic risk zones.

Above the basement highs that act as indentors, the GPS velocity is relatively small compared with the other parts of Taiwan (Fig. 7). The basement highs (Fig. 2) are rooted in the passive margin and thus are relatively stationary with respect to the stable Asian continent. As a result, there are very small strain rates in the basement high regions, but there are relatively large interseismic strain rates along the thrusts right next to the basement highs (Hu et al., 1997; Hsu et al., 2009).

The basement highs are composed of denser materials than the sedimentary strata, and this should be reflected by positive Bouguer gravity anomalies. We found that the two basement highs are clearly visible in the Taiwan Bouguer gravity anomaly map (Fig. 8). As a result, the Chi-Chi main shock is identified as having ruptured in the low-gravity region (blue color) between the two gravity highs.

Heat flow is low above the indentors, but high in front (east) of the indentors (Fig. 9). The higher heat flow might be related to shortening and exhumation or it might be related to the more active dewatering in these zones. There is an active upward gas- and fluid-migration process east of the indentors (e.g., Yang et al., 2006). Similar active deformation is also operating in the fold-and-thrust belt between the indentors.

We found that combined analyses of GPS, gravity, and heat-flow data sets can help to identify the basement highs that act as indentors. For other collision zones around the world, it might be interesting to study regions with similar geophysical features to better explore their seismic risks. In the collision zone, the rapid erosion on the mountains and sedimentation on the continental shelf and slope might have buried some young structures near the frontal thrust region. As a result, these high seismic risk zones might be located near where the geomorphic features are relatively flat and show less surface expression. Seismology, GPS, and gravity observations need to be combined with field observations to better understand the seismic risks in such regions.

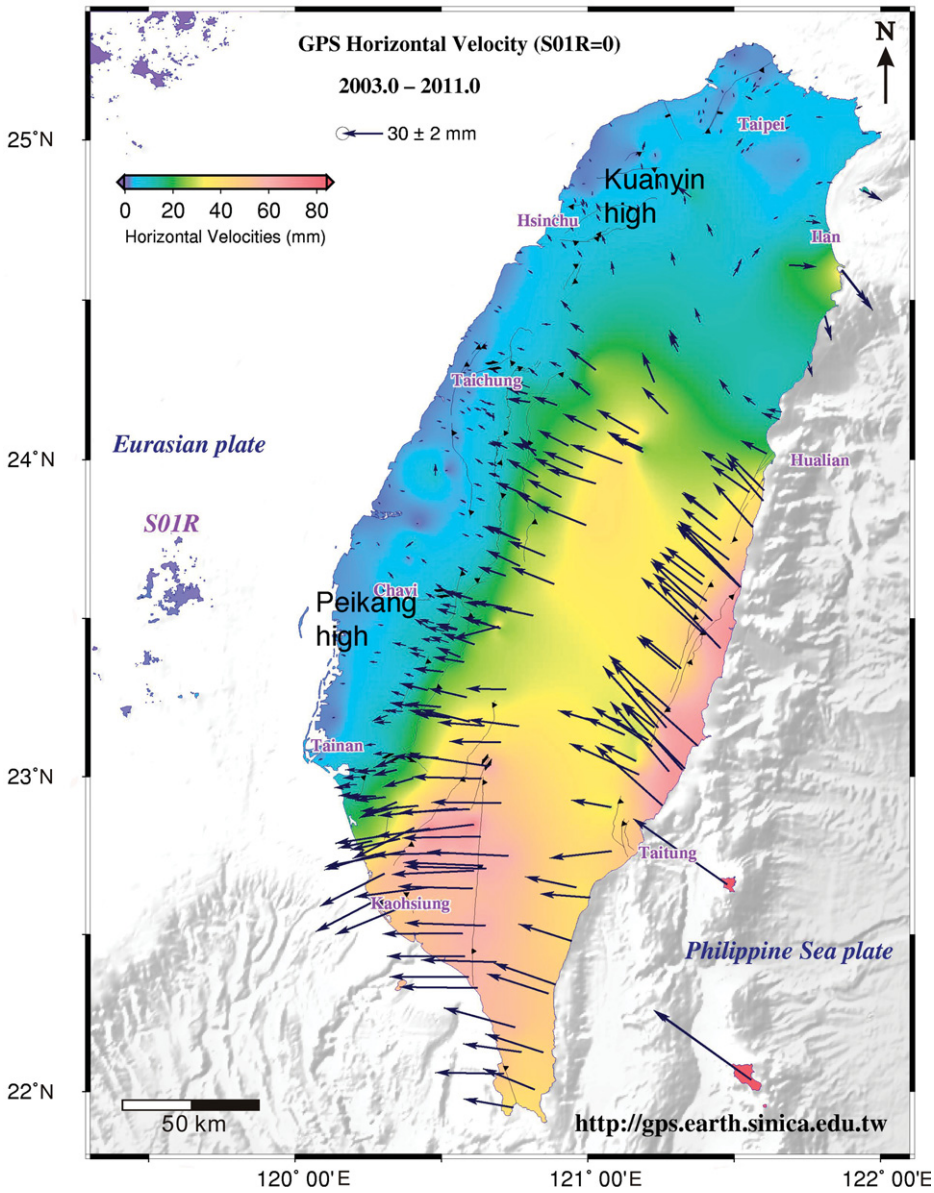

Figure 7. Horizontal displacements of global positioning system (GPS) stations with respect to the stable Asian continent between 2003 and 2009. The two basement highs have very little displacements and can act as indentors coming into the convergent boundary. There are increased displacements east of the indentors in regions where the spacing of the thrusts decreases. The GPS data set was provided by L.C. Kuo in the GPS group at the Institute of Earth Sciences, Academia Sinica.

CONCLUSIONS

The dense population in Taiwan makes dense seismic instrumentation necessary. We used the excellent seismic waveform data sets to invert for seismogenic structures using some state-of-the-art methods. The technical aspects of these methods and initial results have recently been published in earthquake seismology literature. Here, I use the results from these studies to study the seismogenic structures of this region. This is among the most closely seismic-monitored

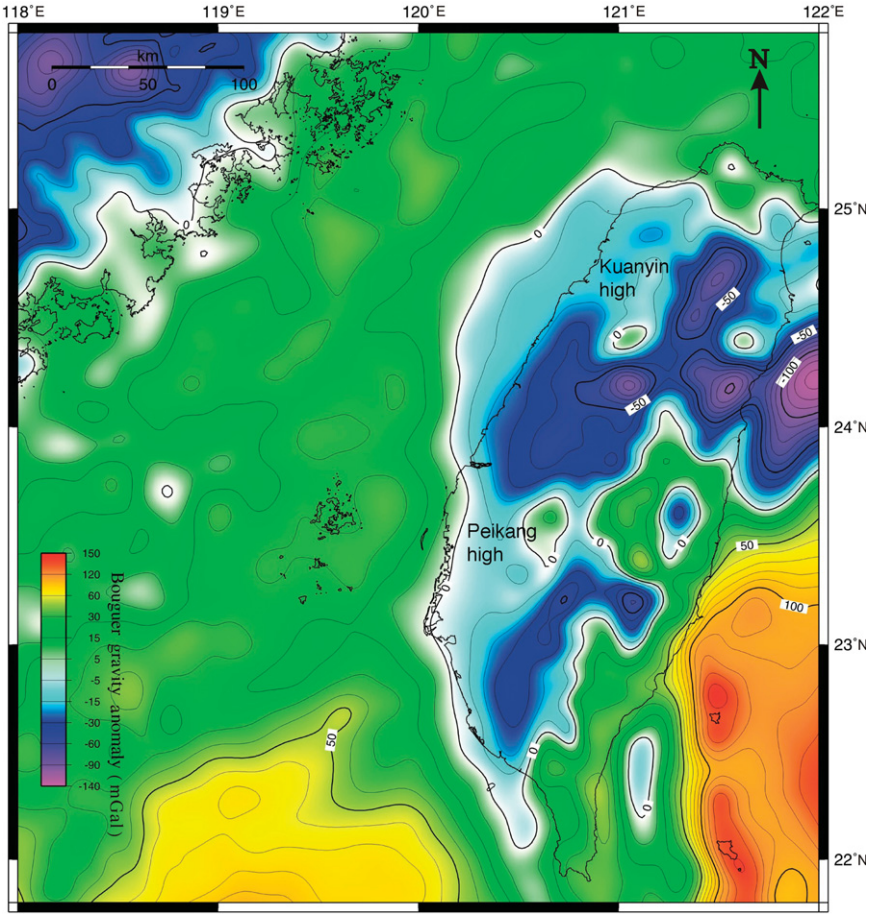

Figure 8. Regional Bouguer gravity anomaly, which is related to the density structures at greater depths. The data set is based on Hsu et al. (1998). The basement highs contain higher-density materials and show up as high-gravity-anomaly regions. The three magnitude 7 earthquakes that ruptured in the past century have slips in the low-gravity-anomaly regions.

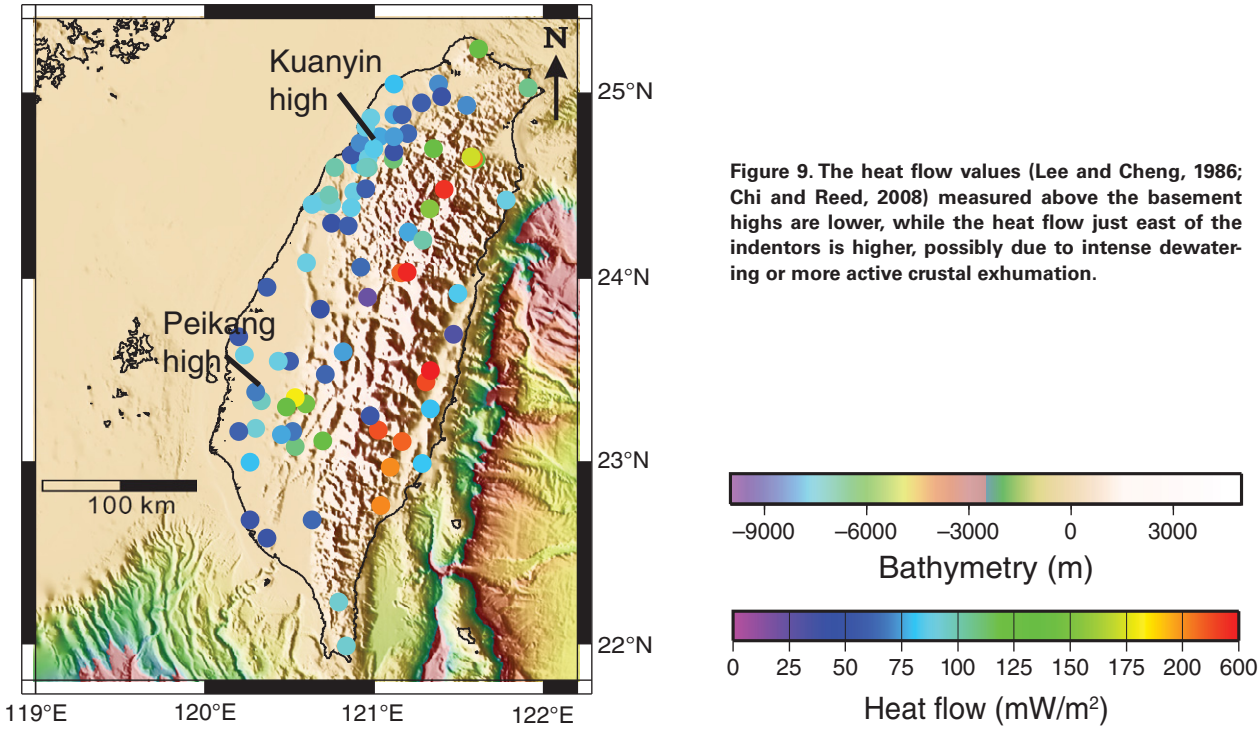

Figure 9. The heat flow values (Lee and Cheng, 1986; Chi and Reed, 2008) measured above the basement highs are lower, while the heat flow just east of the indentors is higher, possibly due to intense dewatering or more active crustal exhumation.

collisional regions with the most comprehensive coseismic energy release data sets in the world. In addition, the oblique convergence in Taiwan region makes subduction and collisional processes occur simultaneously along the convergence zone. We can thus study the range of seismogenic behavior where subduction terminates.

In the collision zone where the "typical" subduction process terminates, the irregular basement topography along the passive margin influences the deformation style (Fig. 10). There is more strike-slip faulting in the collision zone. The horsts on the passive margin that enter into the convergence zone can act as indentors and cause coseismic tectonic extrusion. Here, I have documented coseismic tectonic extrusion deformation on both sides of one indentor, which has generated very high seismic risks near these extrusion regions. I also documented characteristics of GPS, gravity, and heat-flow patterns near these seismogenic zones. The lessons learned from this region might be applied to other ongoing or matured arc-continent collision zones where seismogenic structures are difficult to study.

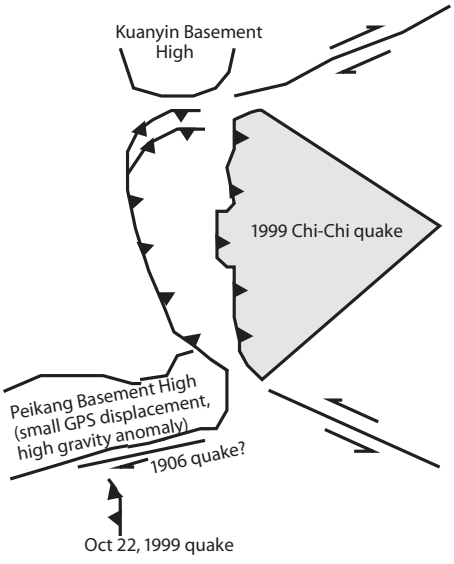

Figure 10. The coseismic tectonic extrusion model proposed in this study. The two basement highs act as indentors squeezing the sedimentary strata in between during the Chi-Chi main shock. One month after the Chi-Chi earthquake, the 22 October 1999 Meishan earthquake sequence occurred on the reverse fault and the strike-slip transfer fault south of the Peikang high. The indentors have small global positioning system displacements, a large Bouguer gravity anomaly, and low heat flow. The shallow thrust (Chi-Chi earthquake) ruptured in a low-gravity-anomaly region. Similar seismogenic structures might exist in other oblique arc-continent collision zones, which might have similar geophysical and geological features.

ACKNOWLEDGMENTS

I thank John Wakabayashi and Science Editor Raymond M. Russo for the great editorial work. I also appreciate two reviewers for the helpful comments. I wish to thank many of my colleagues who made this work possible. This research is partially funded by National Science Council of Taiwan under grant 101-2116-M-001-024 to WCC. This is Contribution Number IESAS1719 of the Institute of Earth Sciences. This is Taiwan Earthquake Center contribution 00085.

REFERENCES CITED

Abers, G.A., and McCaffrey, R., 1994, Active arc-continent collision: Earthquakes, gravity anomalies, and fault kinematics in the Huon-Finisterre collision zone, Papua New Guinea: Tectonics, v. 13, no. 2, p. 227–245, doi:10.1029/93TC02940.

Bowin, C., Lu, R.-S., Lee, C.-S., and Schouten, H., 1978, Plate convergence and accretion in Taiwan-Luzon region: The American Association of Petroleum Geologists Bulletin, v. 62, no. 9, p. 1645–1672.

Briais, A., Patriat, P., and Tapponnier, P., 1993, Updated interpretation of magnetic anomalies and seafloor spreading stages in the South China Sea: Implications for the Tertiary tectonics of Southeast Asia: Journal of Geophysical Research, v. 98, no. B4, p. 6299–6328, doi:10.1029/92JB02280.

Brown, D., Juhlin, C., Alvarez-Marron, J., Perez-Estaun, A., and Oslianski, A., 1998, Crustal-scale structure and evolution of an arc-continent collision zone in the southern Urals, Russia: Tectonics, v. 17, no. 2, p. 158–171, doi:10.1029/98TC00129.

Byrne, T., and Liu, C.S., 2002, Preface: Introduction to the geology and geophysics of Taiwan, *in* Byrne, T., and Liu, C.S., eds., Geology and Geophysics of an Arc-Continent Collision, Taiwan: Geological Society of America Special Paper 358, p. v–vii.

Byrne, T., Chan, Y.C., Rau, R.J., Lu, C.Y., Lee, Y.H., and Wang, Y.J., 2011, The arc-continent collision in Taiwan, *in* Brown, D., and Ryan, P.D., eds., Arc-Continent Collision: Frontiers in Earth Sciences: Berlin, Springer-Verlag, doi:10.1007/978-3-540-88558-0_8.

Carena, S., Suppe, J., and Kao, H., 2002, The active detachment of Taiwan illuminated by small earthquakes and its control of first-order topography: Geology, v. 30, no. 10, p. 935–938, doi:10.1130/0091-7613(2002)030<0935:ADOTIB>2.0.CO;2.

Chang, K.W., Chi, W.C., Gung, Y.C., Dreger, D., Lee, H.K., and Chiu, H.C., 2011, Moment tensor inversions using strong motion waveforms of Taiwan TSMIP data, 1993–2009: Tectonophysics, v. 511, p. 53–66, doi:10.1016/j.tecto.2011.08.020.

Chi, Wu-Cheng, and Dreger, D., 2002, Finite fault inversion of the September 25, 1999 (Mw = 6.4), Taiwan, earthquake: Implications for GPS displacements of Chi-Chi, Taiwan earthquake sequence: Geophysical Research Letters, v. 29, no. 14, doi:10.1029/2002GL015237.

Chi, Wu-Cheng, and Dreger, D., 2004, Crustal deformation in Taiwan: Results from finite source inversions of six Mw >5.8 Chi-Chi aftershocks: Journal of Geophysical Research, v. 109, B07305, doi:10,1029/2003JB002606.

Chi, Wu-Cheng, and Reed, D., 2008, Evolution of shallow, crustal thermal structure from subduction to collision: An example from Taiwan: Geological Society of America Bulletin, v. 120, no. 5/6, p. 679–690, doi:10.1130/B26210.1.

Chi, Wu-Cheng, Dreger, D., and Kaverina, A., 2001, Finite source modeling of the 1999 Taiwan (Chi-Chi) earthquake derived from a dense strong motion network: Bulletin of the Seismological Society of America, v. 91, no. 5, p. 1144–1157, doi:10.1785/0120000732.

Chi, Wu-Cheng, Reed, D., Moore, G., Nguyen, T., Liu, C.S., and Lundberg, N., 2003, Tectonic wedging along the rear of the offshore Taiwan accretionary prism: Tectonophysics, v. 374, p. 199–217.

Dilek, Y., Imamverdiyev, N., and Altunkaynak, S., 2010, Geochemistry and tectonics of Cenozoic volcanism in the Lesser Caucasus (Azerbaijan) and the peri-Arabian region: Collision-induced mantle dynamics and its magmatic fingerprint: International Geology Review, v. 52, no. 4–6, p. 536–578, doi:10.1080/00206810903360422.

Draut, A., and Clift, P., 2001, Geochemical evolution of arc magmatism during arc-continent collision, South Mayo, Ireland: Geology, v. 29, p. 543–546, doi:10.1130/0091-7613(2001)029<0543:GEOAMD>2.0.CO;2.

Houseman, G., and England, P., 1993, Crustal thickening versus lateral expulsion in the India-Asian continental collision: Journal of Geophysical Research, v. 98, no. B7, p. 12,233–12,249, doi:10.1029/93JB00443.

Hsu, S.K., Liu, C.S., Shyu, S.T., Liu, S.Y., Sibuet, J.-C., Lallemand, S., Wang, C., and Reed, D., 1998, New gravity and magnetic anomaly maps in the Taiwan-Luzon region and their preliminary interpretation: Terrestrial, Atmospheric and Oceanic Sciences, v. 9, no. 3, p. 509–532.

Hsu, S.K., Yeh, Y.C., Doo, W.B., and Tsai, C.H., 2004, New bathymetry and magnetic lineations identifications in the northernmost South China Sea and their tectonic implications: Marine Geophysical Researches, v. 25, p. 29–44, doi:10.1007/s11001-005-0731-7.

Hsu, Y.J., Yu, S.B., Simons, M., Kuo, L.C., and Chen, H.Y., 2009, Interseismic crustal deformation in the Taiwan plate boundary zone revealed by GPS observations, seismicity, and earthquake focal mechanisms: Tectonophysics, v. 479, p. 4–18.

Hu, J.C., Angelier, J., and Yu, S.B., 1997, An interpretation of the active deformation of southern Taiwan based on numerical simulation and GPS studies: Tectonophysics, v. 274, p. 145–169, doi:10.1016/S0040-1951(96)00302-2.

Kao, H., and Chen, W.P., 2000, The Chi-Chi earthquake sequence: Active, out-of-sequence thrust faulting in Taiwan: Science, v. 288, p. 2346–2349, doi:10.1126/science.288.5475.2346.

Kao, H., Gao, R., Rau, R.J., Shi, D., Chen, R.Y., Guan, Y., and Wu, F., 2001, Seismic image of the Tarim basin and its collision with Tibet: Geology, v. 29, p. 575–578, doi:10.1130/0091-7613(2001)029<0575:SIOTTB>2.0.CO;2.

Lee, C.R., and Cheng, W.T., 1986, Preliminary heat flow measurements in Taiwan, *in* Proceedings of the Fourth Circum-Pacific Energy and Mineral Resources Conference: Singapore, Circum-Pacific Council for Energy and Mineral Resources, p. 1–9.

Lee, T.-Q., Kissel, C., Barrier, E., Laj, C., and Chi, W.-R., 1991, Paleomagnetic evidence for a diachronic clockwise rotation of the Coastal Range, eastern Taiwan: Earth and Planetary Science Letters, v. 104, no. 2–4, p. 245–257.

Lin, A.T., Watts, A.B., and Hesselbo, S.P., 2003, Cenozoic stratigraphy and subsidence history of the South China Sea margin in the Taiwan region: Basin Research, v. 15, p. 453–478, doi:10.1046/j.1365-2117.2003.00215.x.

Lin, C.H., and Roecker, S.W., 1993, Deep earthquakes beneath central Taiwan: Mantle shearing in an arc-continent collision: Tectonics, v. 12, no. 3, p. 745–755, doi:10.1029/92TC02812.

Liu, C.S., Huang, I.L., and Teng, L.S., 1997, Structural features off southwestern Taiwan: Marine Geology, v. 137, p. 305–319, doi:10.1016/S0025-3227(96)00093-X.

Lu, C.-Y., Chu, H.-T., Lee, J.-C., Chan, Y.-C., and Chang, K.-J., 2002, The 1999 Chi-Chi Taiwan earthquakes and basement impact thrust kinematics: Western Pacific Earth Sciences, v. 2, p. 183–192.

Lundberg, N., Reed, D.L., Liu, C.-S., and Lieske, J., Jr., 1997, Forearc-basin closure and arc accretion in the submarine suture zone south of Taiwan: Tectonophysics, v. 274, p. 5–23.

Malavieille, J., and Trullenque, G., 2009, Consequences of continental subduction on forearc basin and accretionary wedge deformation in SE Taiwan: Insights from analogue modeling: Tectonophysics, v. 466, p. 377–394, doi:10.1016/j.tecto.2007.11.016.

Malavieille, J., Lallemand, S.E., Dominguez, S., Deschamps, A., Lu, C.-Y., Liu, C.-S., Schnurle, P., and the ACT Scientific Crew, 2002, Arc-continent collision in Taiwan: New marine observations and tectonic evolution, *in* Byrne, T.B., and Liu, C.-S., eds., Geology and Geophysics of an Arc-Continent Collision, Taiwan: Geological Society of America Special Paper 358, p. 187–211.

McIntosh, K., Nakamura, Y., Wang, T.K., Shih, R.C., Chen, A., and Liu, C.S., 2005, Crustal-scale seismic profiles across Taiwan and the western Philippine Sea: Tectonophysics, v. 401, p. 23–54, doi:10.1016/j.tecto.2005.02.015.

Nissen, S.S., Hayes, D.E., Yao, B., Zeng, W., Chen, Y., and Nu, X., 1995, Gravity, heat flow, and seismic constraints on the processes of crustal extension: Northern margin of the South China Sea: Journal of Geophysical Research, v. 100, no. B11, p. 22,447–22,483, doi:10.1029/95JB01868.

Peltzer, G., and Tapponnier, P., 1988, Formation and evolution of strike-slip faults, rifts, and basins during the India-Asia collision: An experimental approach: Journal of Geophysical Research, v. 93, no. B12, p. 15,085–15,117, doi:10.1029/JB093iB12p15085.

Reed, D.L., Lundberg, N., Liu, C.S., and Kuo, B.Y., 1992, Structural relations along the margins of the offshore Taiwan accretionary wedge: Implication for accretion and crustal kinematics: Acta Geologica Taiwanica, v. 30, p. 105–122.

Shyu, J.B.H., Sieh, K., Chen, Y.G., and Liu, C.S., 2005, The neotectonic architecture of Taiwan and its implications for future large earthquakes: Journal of Geophysical Research, v. 110, B08402, doi:10.1029/2004JB003251.

Silver, E., Reed, D., McCaffrey, R., and Joyodiwiryo, Y., 1983, Back arc thrusting in the eastern Sunda Arc, Indonesia: A consequence of arc-continent collision: Journal of Geophysical Research, v. 88, no. B9, p. 7429–7448, doi:10.1029/JB088iB09p07429.

Suppe, J., 1984, Kinematics of arc-continent collision, flipping of subduction, and back-arc spreading near Taiwan, *in* Tsan, S.F., Lee, C.-S., Chen, J.C., Chen, C.H., and Pan, K.-L., eds., Geological Society of China Memoir 6, p. 21–33.

Teng, L.S., 1990, Geotectonic evolution of late Cenozoic arc-continent collision in Taiwan: Tectonophysics, v. 183, p. 57–76, doi:10.1016/0040-1951(90)90188-E.

Tsumura, N., Komada, N., Sano, J., Kikuchi, S., Yamamoto, S., Ito, T., Sato, T., Miyauchi, T., Kawamura, T., Shishikura, M., Abe, S., Sato, H., Kawanaka, T., Suda, S., Higashinaka, M., and Ikawa, T., 2009, A bump on the upper surface of the Philippine Sea plate beneath the Boso Peninsula, Japan, inferred from seismic reflection surveys: A possible asperity of the 1703 Genroku earthquake: Tectonophysics, v. 472, p. 39–50, doi:10.1016/j.tecto.2008.05.009.

Wang, K., and Bilek, S.L., 2011, Do subducting seamounts generate or stop large earthquakes?: Geology, v. 39, no. 9, p. 819–822, doi:10.1130/G31856.1.

Wang, T.K., Chen, M.K., Lee, C.S., and Xia, K., 2006, Seismic imaging of the transitional crust across the northeastern margin of the South China Sea: Tectonophysics, v. 412, p. 237–254, doi:10.1016/j.tecto.2005.10.039.

Willett, S.D., Fisher, D., Fuller, C., Yeh, E.C., and Lu, C.Y., 2003, Erosion rates and orogeny-wedge kinematics in Taiwan inferred from fission-track thermochronometry: Geology, v. 31, p. 945–948, doi:10.1130/G19702.1.

Wu, F., Rau, R.J., and Salzberg, D., 1997, Taiwan orogeny: Thin-skinned or lithospheric collision?: Tectonophysics, v. 274, p. 191–220, doi:10.1016/S0040-1951(96)00304-6.

Yang, T.F., Fu, C.C., Walia, V., Chen, C.H., Chyi, L.L., Liu, T.K., Song, S.R., Lee, M., Lin, C.W., and Lin, C.C., 2006, Seismo-geochemical variations in SW Taiwan: Multi-parameter automatic gas monitoring results: Pure and Applied Geophysics, v. 163, p. 693–709, doi:10.1007/s00024-006-0040-3.

Yen, J.Y., and Lundberg, N., 2006, Sediment compositions in offshore southern Taiwan and their relations to the source rocks in modern arc-continent collision zone: Marine Geology, v. 225, p. 247–263, doi:10.1016/j.margeo.2005.09.003.

Yu, S.B., Chen, H.Y., and Kuo, L.C., 1997, Velocity field of GPS stations in the Taiwan area: Tectonophysics, v. 274, p. 41–59, doi:10.1016/S0040-1951(96)00297-1.

MANUSCRIPT RECEIVED 16 DECEMBER 2011
REVISED MANUSCRIPT RECEIVED 30 JULY 2012
MANUSCRIPT ACCEPTED 2 AUGUST 2012

Printed in the USA